Three-dimensional Finite Element Analyses of Barrette Piles under Compression and Uplift Loads with Field Data Assessments

D.W. Chang[1], C. Lin[2], T.Y. Wang[3], Y.K. Lin[4], F.C. Lu[5] and C.J. Kuo[6]
[1,2,3]*Department of Civil Engineering, Tamkang University, Tamsui, New Taipei City, Taiwan*
[4,5,6]*Ground Master Construction / MICE Engineering Consultants, Taipei, Taiwan*
*E-mail:*dwchang@mail.tku.edu.tw

ABSTRACT: This paper presents the three-dimensional finite element modeling of barrette piles in clayey and sandy soils, in which the piles are subjected to statically compressive and uplift loads. Load displacement curves and load transfers were monitored and compared to solutions from one-dimensional finite difference analysis. Capacities of the barrette piles were examined by interpretation methods and bearing capacity equations. Pile load test data of barrette piles located in Xingyi District, Taipei Basin was used for simulation. It was found that the conventional bearing capacity equations are applicable to barrette piles. The interface elements between pile and soils were found to significantly affect the results. Finite element analysis can provide more complete solutions when compared with finite difference analysis. It was also found that the soil frictions due to pile uplift in soft clays at Taipei Basin were underestimated when using common strength reduction ratios.

KEYWORDS: Barrette pile, Finite element analysis, Finite difference analysis, Pile load test, Interpretation method

1. INTRODUCTION

Barrette piles have been used in engineering practice in Taiwan for many years. There are a number of building foundations that have been constructed using barrette piles (Hsu, 2017). In general, the design of barrette piles follows conventional pile design methods. Axial capacity of the pile can be estimated assuming that the frictions and end resistance of the pile are fully mobilized. In addition, pile load tests can be conducted to examine the capacities obtained from the calculations (Fellenius, 1980, 1984, 1999a, 1999b). To simulate the load-displacement mechanism of a single pile under axial loads, Reese and his associates had proposed the APILE analysis in the 1980s (Wang *et al.*, 2018). The so called *t-z* and *q-z* curves representing the load transfers between shaft and soils, as well as those at the pile tip have been suggested based on field experiments. When a series of *t-z* springs are attached to the pile segments, with proper boundary values the pile load mechanism can be monitored using the finite difference scheme. This type of numerical solution has been used popularly in engineering design practice (Fellenius, 1989, 1998). As to the lateral capacity of the barrette pile, available analyses such as the analytical formulations suggested by Chang (1937) or the one-dimensional finite difference analysis (FDA), LPILE proposed by Reese and his colleagues in 1980s (Isenhower *et al.*, 2018) can be used. The so called *p-y* curves were suggested in the lateral case to simulate the load transfers along the pile shaft. In order to examine the nonlinear performance of the concrete pile, the push-over test is often conducted to evaluate the moment and shear capacities of the pile. Although the above simplified analyses have been popularly used in design practice, more rigorous computer-based analyses such as the finite element method, have been utilized in engineering practice in recent years (Poulos, 2001).

This study discusses the barrette pile mechanism subjected to compression and uplift loads, using the three-dimensional finite element analysis (FEA) based on the Midas-GTS NX program (Midas, 2014). Numerical models of a single barrette pile located in clayey and sandy layers were examined. The Mohr-Coulomb model was presumed for soils, and the concrete barrette pile was assumed to be linearly elastic. Interface elements were used to simulate the frictions between pile and soils. Because the pile will experience cracking when subjected to the uplift loads, the pile stiffness was varied initially along the shaft to produce more realistic results. The load-displacement curves, the axial loads and frictions varying along the pile, and the *t-z*/*q-z* relations associated with the FEA were compared with those from the APILE analysis. The capacities of the numerical models were then reported using various interpretation methods, and were subsequently compared to those obtained from hand calculations using bearing capacity equations. The pile load data of a couple of the testing piles at a site located in the Xingyi district, Taipei Basin were adopted in this study. Again, the FEA was used to model the field data, and the solutions were compared with those from APILE analysis. Pile capacities were then estimated using interpretation methods, and were then compared with those obtained from hand calculations. Details of the observations are discussed next.

2. METHODOLOGIES

2.1 Midas-GTS NX Analysis

Finite element analysis has gained popularity in the design of geotechnical structures since the 2000s. It has been known as the most effective tool among the rigorous computer-based methods available (Poulos, 2001; Abderlrazaq *et al.*, 2011). There are many computer packages available at present. For instance, Midas-GTS NX was made by Midas Co. (Midas, 2014) for geotechnical engineering work. It has recently been adopted by Chang *et al.*, (2018) and Chang and Lien (2018) for the use of comparison with the newly developed WERAFT-S and WEAPRF-S programs for raft foundation and piled raft foundations, respectively. The functions of the Midas-GTS NX analysis are similar to other geotechnical engineering software such as PLAXIS, FLAC, etc. The three-dimensional FE analysis can provide any displacement component at the nodes of the structural system. It can further reveal the stresses at the nodes, and any of the elements. However, it should be noted that the stresses revealed at the nodes need to be carefully used. The Midas-GTS NX analysis is the main tool used in carrying out this study.

2.2 APILE Analysis

The approximate computer-based methods can provide simplified but effective solutions to the analysis of pile foundations (Poulos, 2001). If the pile foundation was treated as a rigid pile group, then the single pile behaviors should be monitored carefully. With such concerns, the APILE analysis has been suggested in 1980s by Reese and his colleagues (Wang *et al.*, 2018). The analysis was mainly established using the finite difference (FD) formulas for equilibrium equations of pile segments under vertical loads. A set of soil springs were attached to the pile including pile tip, to simulate the loads transferred to surrounding soils. Frictions and end resistance of the soils were both modeled. The load displacement curves representing the mechanism were called *t-z* and *q-z* curves. The analysis using APILE program was performed by giving a set of prescribed displacements to the pile segments. Total resistance of the pile was obtained by back figuring according to the prescribed displacements. As to the ultimate pile

capacity, the analysis adopts the bearing capacity equations with the assigned soil strength parameters to provide the values. Chang and Yeh (1999) have proposed a similar FD analysis for piles under dynamic loads. A time-dependent damping model has also been suggested by Chang *et al.* (2000) to approximate the energy dissipations throughout the loading history. In this study, APILE analysis has been adopted for comparisons with the Midas-GTS NX analysis.

2.3 Analytic Equations for Pile Capacities

The capacity equations were also used in this study to compute the capacity of single piles. For the compression piles in clay, the equations for the frictions can be calculated using the α method (Tomlinson, 1971), λ method (Vijayvergiya and Focht, 1972), and AASHTO method (2002). The end bearing resistance can be estimated by S_uN_c, which assumes that the clay is in undrained condition, where S_u is the undrained shear strength of the clay and N_c is the bearing capacity coefficient. For compression piles in sands, the frictions of the piles can be computed using the equations suggested by Meryerhof (1976) and AASHTO method (2002). The end resistance of the pile can be approximated by $\sigma_v'N_q$, where σ_v' is the effective stress at pile tip and N_q the bearing capacity coefficient.
When the pile is subjected to uplift loads, end resistance of the pile can be neglected, only the frictions are taken into account. If the piles are in clay soils, one can refer to the methods suggested by Das and Seeley (1982) and AASHTO (2002). For piles in sands, the frictions can be calculated using the method proposed by Meyerhof and Adam (1968) and AASHTO (2002). The equations suggested by AASHTO method are very similar to those for compression piles but with a 30% reduction. The weight of the concrete pile needs to be included in the uplift case. Details of the above methods to compute the frictions and end bearings can be found in Lin (2018).

2.4 Interpretations of Pile Load Test Data

For the pile load test data used, many interpretation methods are available to examine the vertical capacity of pile. A summary of the commonly used methods was suggested by Fellenius (1980). In general, the methods can be divided into three categories: 1. Settlement control method, which includes Terzaghi method (1942), Canadian method (1985), AASHTO method (2002), and Hirany and Kulhawy method (1988), 2. Load-displacement characteristics method, in which Chin method (1970) and the Van der Veen method (1953) are the representatives. 3. Tangent method, in which Davisson method (1972), De Beer method (1967) and Fuller and Hoy method (1970) are the known ones. According to local experiences, Van der Veen method (1953) and Fuller and Hoy method (1970) are mostly used in design practice in Taiwan. All these methods will be adopted to estimate the barrette pile capacities in this study.

3. NUMERICAL MODELLING

The numerical models and the material properties of the barrette piles used in the FEA in this study can be found in Table 1. Clayey and sandy strata were both assumed. Soil stiffness was increased with the layer depth. The effects of the ground water table and pore water movements were neglected in the modeling. Mohr-coulomb failure criterion was assumed for the soils. As shown in the results, clayey soils were dominated by the undrained shear strength. Sandy soils were controlled by the internal friction angles. The internal friction angles of the sandy layers were averaged in the analysis for the interpretations. Linear elastic material was assumed for the concrete piles. However for piles under the uplift loads, the piles were decomposed into five segments where the correspondent stiffness was reduced from top to bottom, to simulate the cracking and deterioration of the pile subjected to uplift loads.

Table 1 Numerical model used in Midas analysis

<table>
<tr><th>Load</th><th>Size of analytical zone</th><th colspan="3">Soil profile and material properties</th><th>Barrette pile dimensions and properties</th></tr>
<tr><td rowspan="9">Comp.</td><td rowspan="9">L×W×H=
60mx60mx
80m</td><td rowspan="5">Clay</td><td>Vs=120m/s, SPT-N=2
Es= 87MPa, Su=50kPa</td><td rowspan="5">h=20m
γ=20
kN/m³
ν= 0.49
φ'= 0°</td><td rowspan="9">2.5mx0.8mx70m
γ_c = 24 kN/m³
E_c = 35000 MPa
ν= 0.13</td></tr>
<tr><td>Vs=200m/s, SPT-N=8,
Es= 240MPa, Su=140kPa</td></tr>
<tr><td>Vs=222m/s, SPT-N=10
Es= 300MPa, Su=170kPa</td></tr>
<tr><td>Vs=237m/s, SPT-N=13
Es= 342MPa, Su=200kPa</td></tr>
<tr><td rowspan="4">Sand</td><td rowspan="4">Vs=150m/s, SPT-N=7
Es= 113MPa, φ'=24°
Vs=249m/s, SPT-N=30
Es= 310MPa, φ'=34°
Vs=278m/s, SPT-N=42
Es= 390MPa, φ'=37°
Vs=297m/s, SPT-N=51
Es= 444MPa, φ'=40°</td><td rowspan="4">h=20m
γ=19
kN/m³
ν= 0.3
Avg.
φ'=35°</td></tr>
<tr><td rowspan="2">Uplift</td><td rowspan="2">L×W×H=
60mx60mx
80m</td><td>Clay</td><td colspan="2">Same as above</td><td rowspan="2">0~2m, Ec =7000MPa
2~10m, Ec =14000MPa
10~20m, Ec =21000MPa
20~40m, Ec =28000MPa
40~70m, Ec =35000MPa
γ_c and ν are the same as above</td></tr>
<tr><td>Sand</td><td colspan="2">Same as above</td></tr>
</table>

For the Midas-GTS analysis, the contact elements between the pile and soils were guided by a simple elastoplastic model. The frictional stiffness (*Kt*) of the contact element was presumed equal to the Young's modulus of the soils (*Es*). For the frictional strength of the element, if the piles were in clays, the adhesions (c_a) between the pile and the soils were related to the undrained shear strength of the clayey soils (S_u). Reduction coefficient (α) of value 0.66 and 0.33 were used to reduce the undrained shear strength (*e.g.*, $c_a=\alpha S_u$) for the compression pile and uplift pile, respectively. For the pile in sandy soils, the frictions between the pile and soils (*f*) were related to the internal friction angle of the soil (ϕ), *i.e.*, $f = \tan\delta = \tan(\beta\phi)$, where β is the reduction coefficient for the internal friction angle. In this study β was assigned as 0.66 and 0.33 respectively for compression and uplift pile.

A uniformly distributed load was applied on top of the barrette pile. 70MN and 30MN were the maximum loads applied for compression and uplift, respectively. In the nonlinear analysis, the load was divided into 10 steps, and the iterative analysis was used to ensure the satisfaction of force equilibrium. The pile was composed of eight, 4-node isoperimetric elements at the same depth. Following the auto-meshing processes in Midas-GTS, the three-dimensional FE mesh consisted mostly of 8-node brick elements and 6-node pentahedrons. Figure 1 shows the typical FEA mesh used in the study. Essential boundary conditions such as roller and hinge were implemented at the FE boundaries. The stability and convergence of the numerical solutions were ensued by enlarging the size of FE zone. Figure 2 depicts the appropriateness of the solutions with respect to the size of the FE zone for pile in clays.

The numerical models and the model parameters of the barrette piles used for APILE analysis are the same as those used in Midas analysis. Maximum friction along the pile and the soil was assumed as 0.66 and 0.33 times the soil strength parameters for compression pile and uplift pile. API method was used for *t-z* and *q-z* curves for comparisons. To simulate the uplift load test, an averaged stiffness of the pile segments was assumed in APILE analysis. The correspondent Young's modulus of the pile was assumed as 27000MPa.

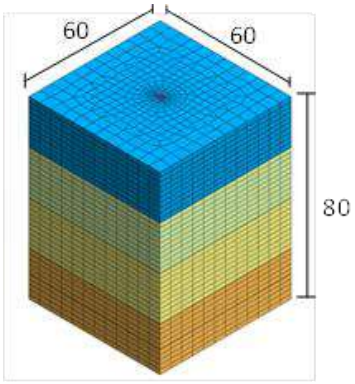

Figure 1 FE mesh used in the Midas analysis

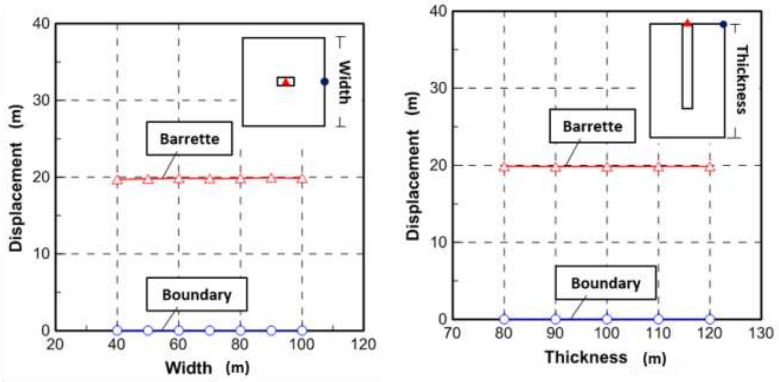

Figure 2 Stability analysis of the analytical FE zone for pile in clays

4. BEHAVIOURS OF MODEL PILES

4.1 Loading Mechanism

The results from FEA modeling on the compression pile in clays are shown in Figure 3. It can be found that the load-displacement curve of the model pile yields at approximately 50MN, while the load developed until a displacement of 20cm. The axial stresses along the pile decreased gradually along the shaft. However, it also found that the axial stresses increased with greater loading. Friction stresses along the pile were also greater with increased loading. The *t-z* curves indicate that the load transfers were dominated mainly by the interface elements. In order for the frictions to be mobilized, the required displacements were found rather small (<0.5cm) regardless of the depth. In the *q-z* curve expressing the behavior of the pile tip, the bearing pressures were found to be much larger than the frictional stresses at a displacement of 0.5cm. As the displacement increased, the stress starts to yield and develops until a displacement of 15cm. Similar FEA solutions for the compression pile in sands are shown in Figure 4. The load-displacement curve for the pile yielded at roughly 40MN. When the load reaches 70MN, only a 6cm displacement was found. The curves for the pile in sands were much stiffer than those in clayey soils. The *t-z* curves for the pile in sandy soils were also found to develop slowly. As the depth increased, it can be seen that the frictions were hard to mobilize. With regards to the *q-z* curves, it was found that only a 0.6cm displacement is required to cause a bearing stress of 7MPa. It should be noted that, the above phenomena are dependent on the model parameters in use.

Results of FEA modeling on the uplift barrette pile in clays are shown in Figure 5. It can be found that the load-displacement curve of the model pile yielded at approximately 25MN, while the ultimate capacity was reached at 30MN for settlement greater than 4cm. The tensile stresses along the pile decreased gradually along the shaft, and increased with greater loading. The frictions along the pile also increased with added load. The *t-z* curves for the pile under the tensile loads are very similar to those subjected the compression loading. However, the displacements are much smaller than those under compression. For solutions of the uplift pile in sands, Figure 6 depicts the results. Similar phenomena can be seen from results obtained for the compression and uplift piles in clay soils.

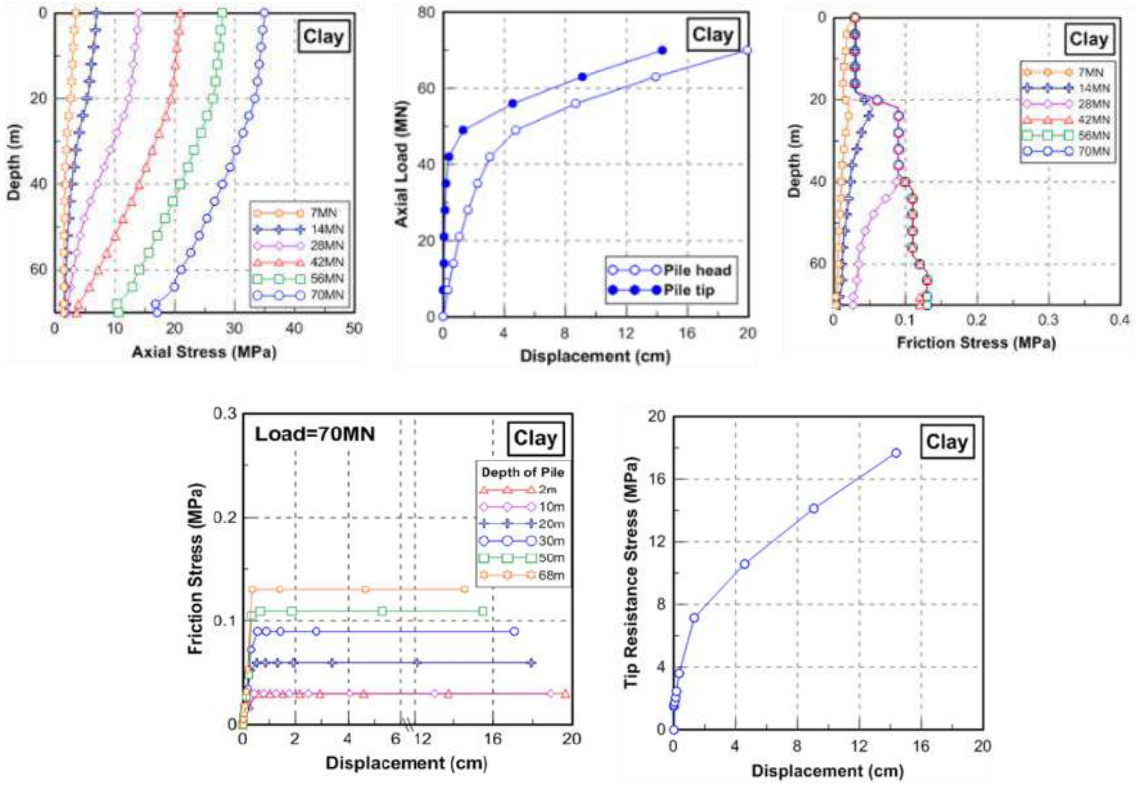

Figure 3 Load beahviors of compression pile in clays

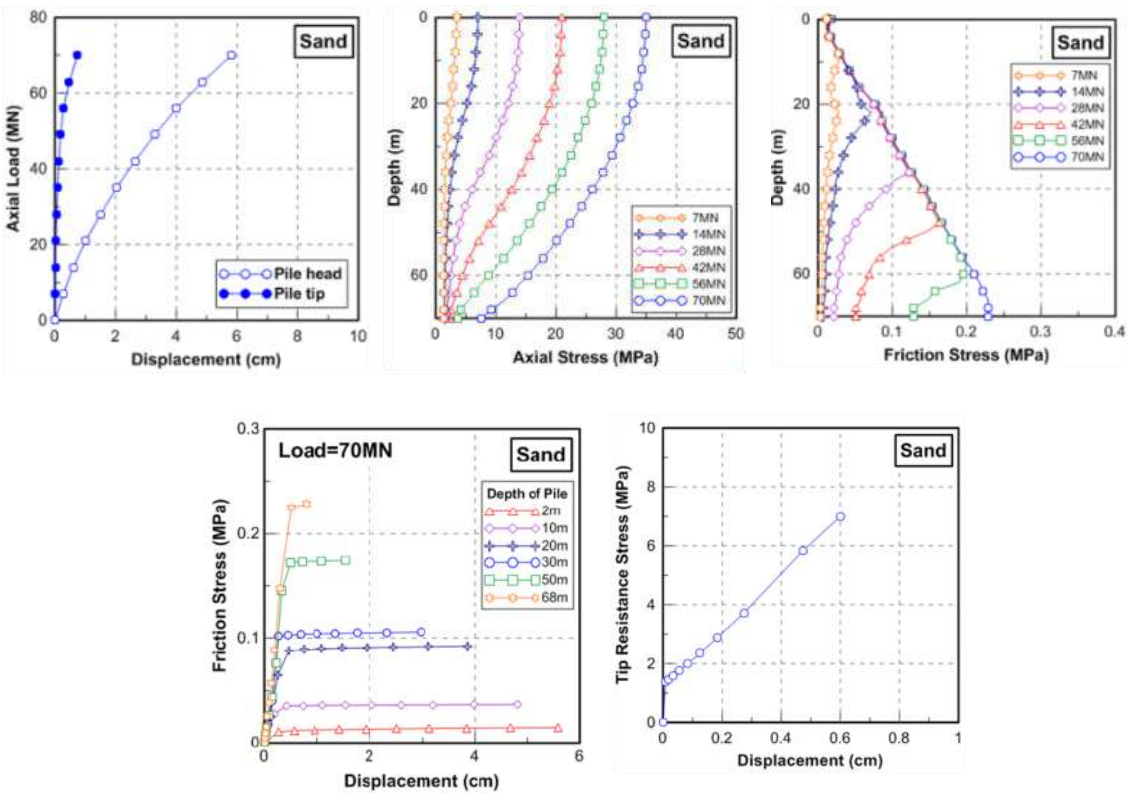

Figure 4 Load beahviors of compression pile in sands

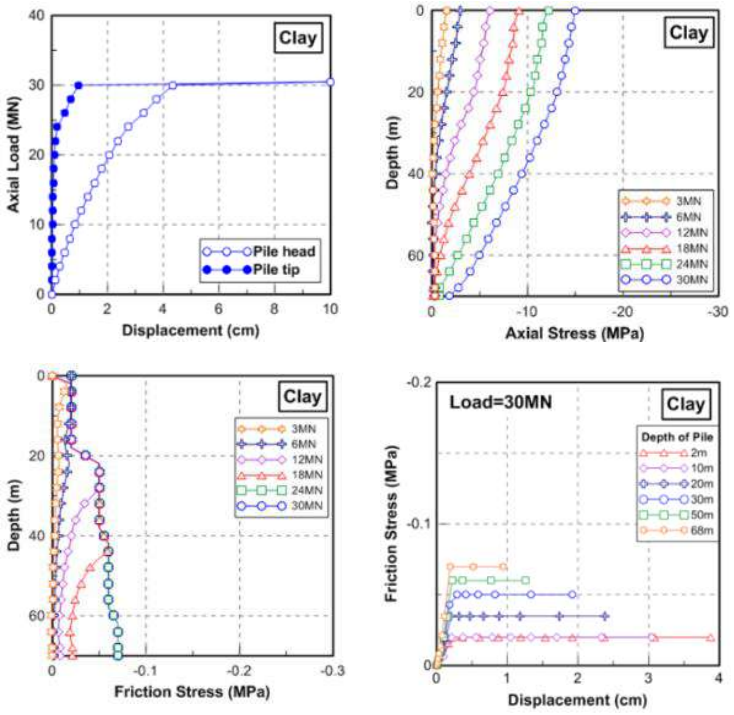

Figure 5 Load beahviors of uplift pile in clays

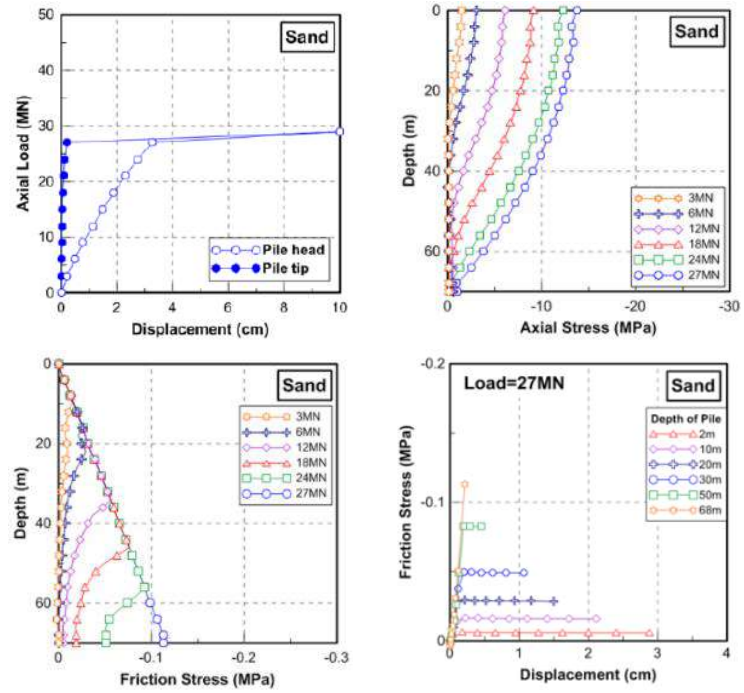

Figure 6 Load beahviors of uplift pile in sands

The effects of the shape of the barrette pile, the strength parameters for the interface frictions (*i.e.*, C_a and δ), and the dilatancy angle (ψ) affecting the compression piles were studied. In general, it was found that the deformations, axial and frictional stresses at both sides of the barrette pile are approximately the same. The adhesion (C_a) and frictional angle (δ) between the pile and the clayey soils are important parameters (Lin, 2018). Figure 7 depicts the influences of the dilatancy angle (ψ) which can simulate the roughness of the contact planes between the pile and the sandy soils, which results in an apparent resistance appearing at the pile head. It was found that at the depth of 0-20m, the frictions were affected by both δ and ψ. For depths greater than 20m, the frictions were mainly controlled by ψ.

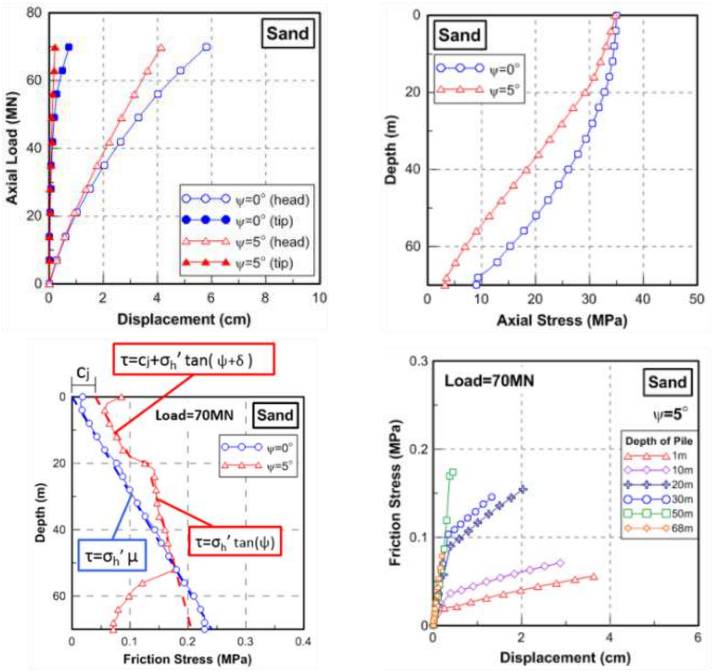

Figure 7 Effects of dilatancy angle used for interface roughness for compression pile in sands

4.2 Pile Capacities from Interpretations

Eight interpretation methods were used to analyze the capacities of the numerical piles. The load-displacement curves shown in Figures 3-6 were used for the interpretations. The results were reported by Lin (2018) for the capacities of the barrette pile model in clayey and sandy soils under compression and uplift loads. Corresponding results for the compression pile in clays and sands are summarized in Table 2 and Table 3. It can be found that for the compression piles in clays, the AASHTO method provides the lowest estimation, whereas the Chin method gives the highest capacity.

Table 2 Pile capacities from interpretation methods, analytic equations and APILE analysis for compression pile in clays

Interpretation method	O_{ult} (MN)	Analytic method	Q_s (MN)	Q_b (MN)	$Q_s + Q_b = Q_{ult}$ (MN)	APILE O_{ult} (MN)
Terzaghi (1942)	**65**	α method	38.45	4.875	**43.32**	**42.62**
Canadian (1985)	**37**					
AASHTO (2002)	**15**	λ method	41.42		**46.29**	
Chin (1970)	**79**					
Van der Veen (1953)	**63**	AASHTO	34.12		**38.99**	
Davisson (1972)	**48**					
De Beer (1967)	**42**	$f_s = c_a$	41.36		**46.23**	
Fuller and Hoy (1970)	**>70**					

Table 3 Pile capacities from interpretation methods, analytic equations and APILE analysis for compression pile in sands

Interpretation method	O_{ult} (MN)	Analytic method	Q_s (MN)	Q_b (MN)	$Q_s + Q_b = Q_{ult}$ (MN)	APILE O_{ult} (MN)
Terzaghi (1942)	**150**	Meyerhof	28.6	50.06	**78.63**	**124.84**
Canadian (1985)	**40**					
AASHTO (2002)	**15**					
Chin (1970)	**285**					
Van der Veen (1953)	**130**	AASHTO	49.19	66.5	**115.69**	
Davisson (1972)	**70**					
De Beer (1967)	**80**	fs= K σ_v' tanδ	56.74		**123.24**	
Fuller and Hoy (1970)	**>200**					

The values reported by the Davisson method were found closest to the averaged values. For the compression pile in sands, the methods which provide the lowest and highest values are similar to those for the pile in clays. The value estimated using Davisson method and De Beer method were found closer to the averaged values. Corresponding graphic results are shown in Figure 8 and Figure 9 for compression piles in clays and sands, respectively.

For the uplift capacities of the numerical pile, the results from the interpretation methods are summarized in Table 4 and Table 5 for the pile in clays and sands, respectively.

Table 4 Pile capacities from interpretation methods, analytic equations and APILE analysis for uplift pile in clays

Interpretation method	O_{ult} (MN)	Analytic method	Q_s (MN)	W_c (MN)	$Q_s + Q_b = Q_{ult}$ (MN)	APILE O_{ult} (MN)
Hirany and Kulhawy (1988)	**14**	Das and Seeley	28.11	3.36	**31.47**	**25.13**
Canadian (1985)	**23**					
AASHTO (2002)	**8**					
Chin (1970)	**57**					
Van der Veen (1953)	**45**	AASHTO	23.89		**27.25**	
Davisson (1972)	**17**					
De Beer (1967)	**21**	$f_s = c_a$	20.68		**24.04**	
Fuller and Hoy (1970)	**>30**					

Table 5 Pile capacities from interpretation methods, analytic equations and APILE analysis for uplift pile in sands

Interpretation method	O_{ult} (MN)	Analytic method	Q_s (MN)	W_c (MN)	$Q_s + Q_b = Q_{ult}$ (MN)	APILE O_{ult} (MN)
Hirany and Kulhawy (1988)	**13**	Meyerhof and Adam	19.8	3.36	**23.16**	**28.89**
Canadian (1985)	**23**					
AASHTO (2002)	**8**					
Chin (1970)	**65**					
Van der Veen (1953)	**55**	AASHTO	34.44		**37.8**	
Davisson (1972)	**15**					
De Beer (1967)	**21**	fs= K σ_v' tanδ	28.25		**31.61**	
Fuller and Hoy (1970)	**>30**					

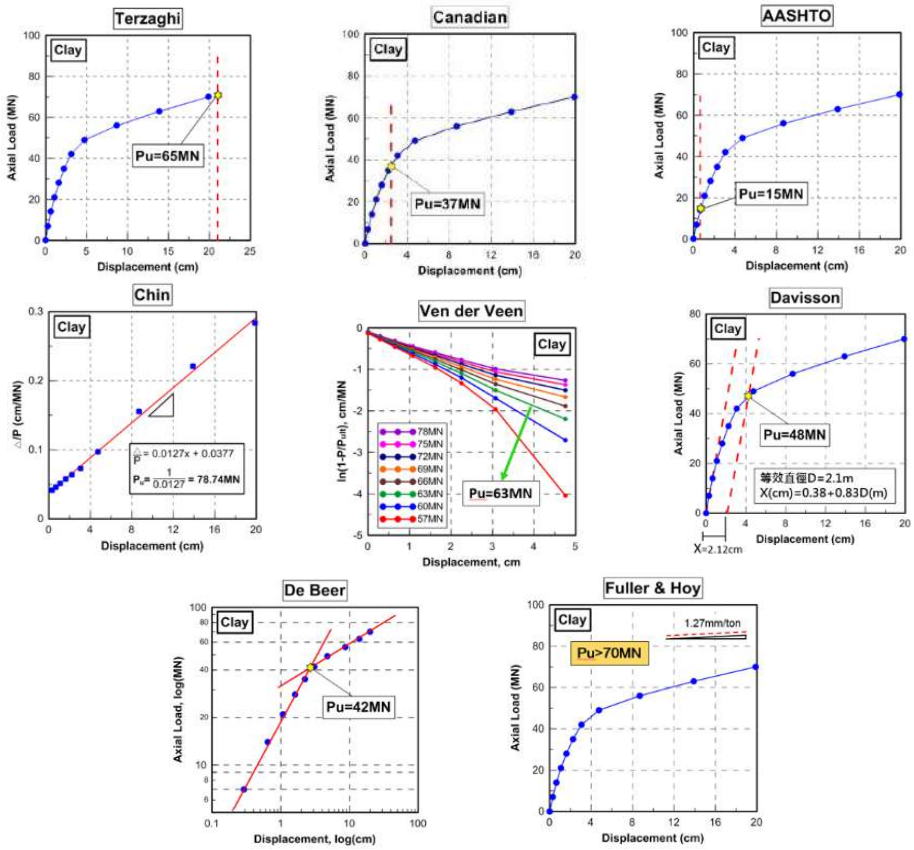

Figure 8 Interpretations of capacity for compression pile in clays

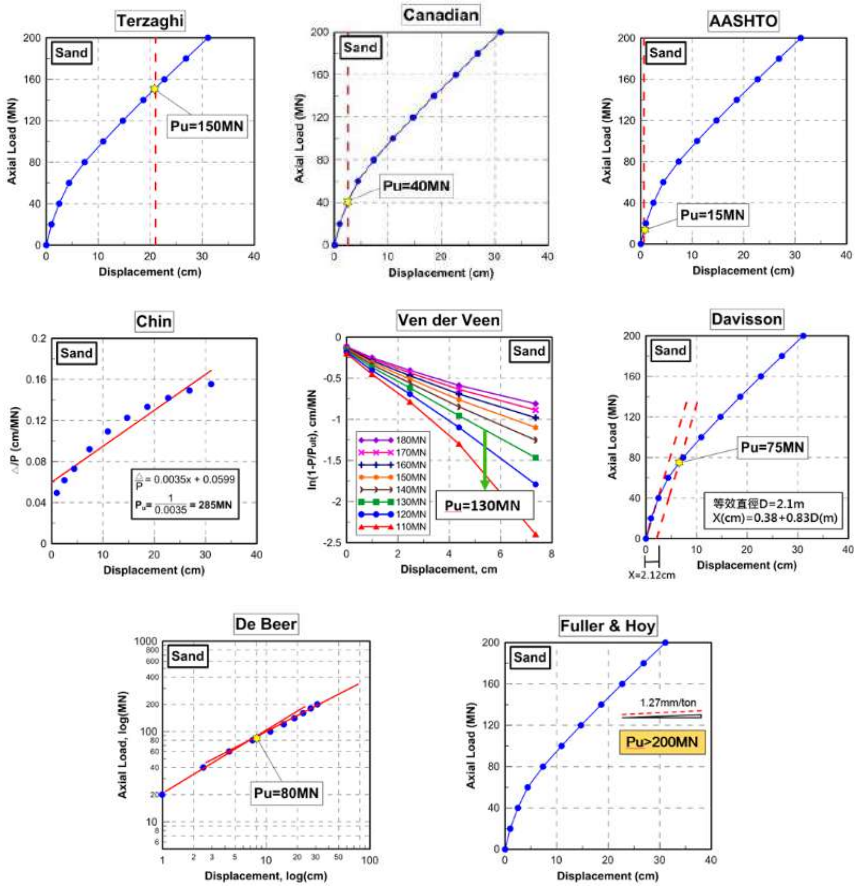

Figure 9 Interpretations of capacity for compression pile in sands

Notice that in this case, the yield capacities of the piles are very similar to the ultimate capacities. In clayey soils, the lowest and highest estimations were found the same as those found in the compression piles. The Canadian method, De Beer method, and Fuller and Hoy method were found to be closer to the averaged values. For the cases in sand, the estimations are similar to those in clay. Corresponding graphic results are shown in Figure 10 and Figure 11 for uplift piles in clays and sands, respectively.

5. COMPARATIVE ANALYSES

5.1 Comparisons on Pile Behaviors

Comparisons of the results from the APILE analysis on the compression pile model in clays and sands are shown in Figure 12 and Figure 13. In Figure 12, it is obvious that the FD analysis yields much less load than the FE analysis. The *t-z c*urves are slightly different, since the API method preserved some softening characteristics. The *q-z* curve obtained by APILE is also found much smaller than FE analysis. Apart from that, the axial and frictional stresses from the FD and FE analyses are found agreeable. In Figure 13, the load displacement curves are found to be agreeable, since the pile resistance is much larger in sands. The FD solution yields at about 60MN, whereas the FE solution develops continuously to the maximum load applied.

The results from the APILE analysis on the numerical piles in clays and sands under the uplift loads are plotted in Figure 14 and Figure 15. For the case of the uplift loads, the results from the FE and FD analyses were found to be compatible. Similar yield phenomena can be found in the load-displacement curves obtained from both methods. In both clayey and sandy layers, the load-displacement starts to yield while the piles were uplifted by 2~4cm.

5.2 Comparison on Pile Capacities

Pile capacities obtained from the interpretations on the load-displacement curves of the compression and uplift piles in clays and sands were compared with those computed using the bearing capacity equations and APILE (Lin, 2018). They are summarized in Tables 2~5. Note that for the compression pile in clays, the solutions from the bearing capacity equations and APILE seem to be closer to the results from the Davisson method, and the De Beer method. For the compression pile in sands, the estimation from Meyerhof equations was found much lower than other calculations. The pile capacity is more attributed to the end bearing of the pile in this case. Significant varieties can be found in the interpretation methods. It was found that, the Van der Veen method was closer to the upper bound of the calculations whereas the Davisson and the De Beer methods were similar to the Meyerhof solution.

With regards to the uplift capacity of the piles in clays and sands, more compatible results were obtained from the interpretation methods, and the calculations from the analytic equations and APLIE analysis. The Canadian and the De Beer methods can both provide results closest to the calculations for the case of the pile in clays, and also in sands.

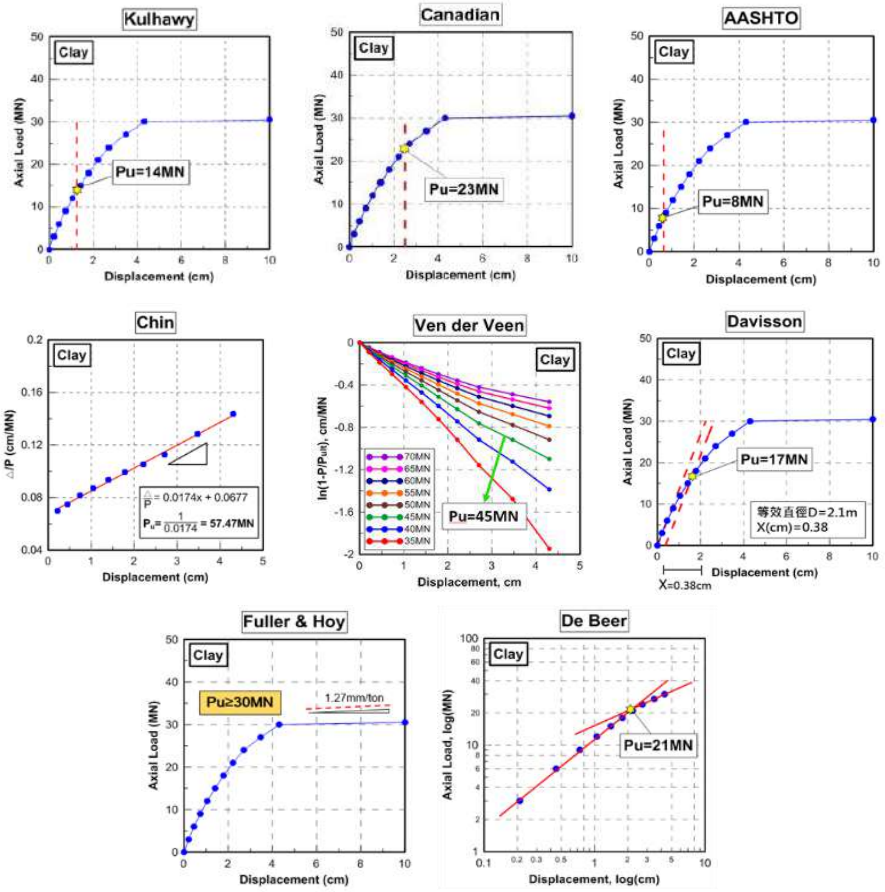

Figure 10 Interpretation of capacity for uplift pile in clays

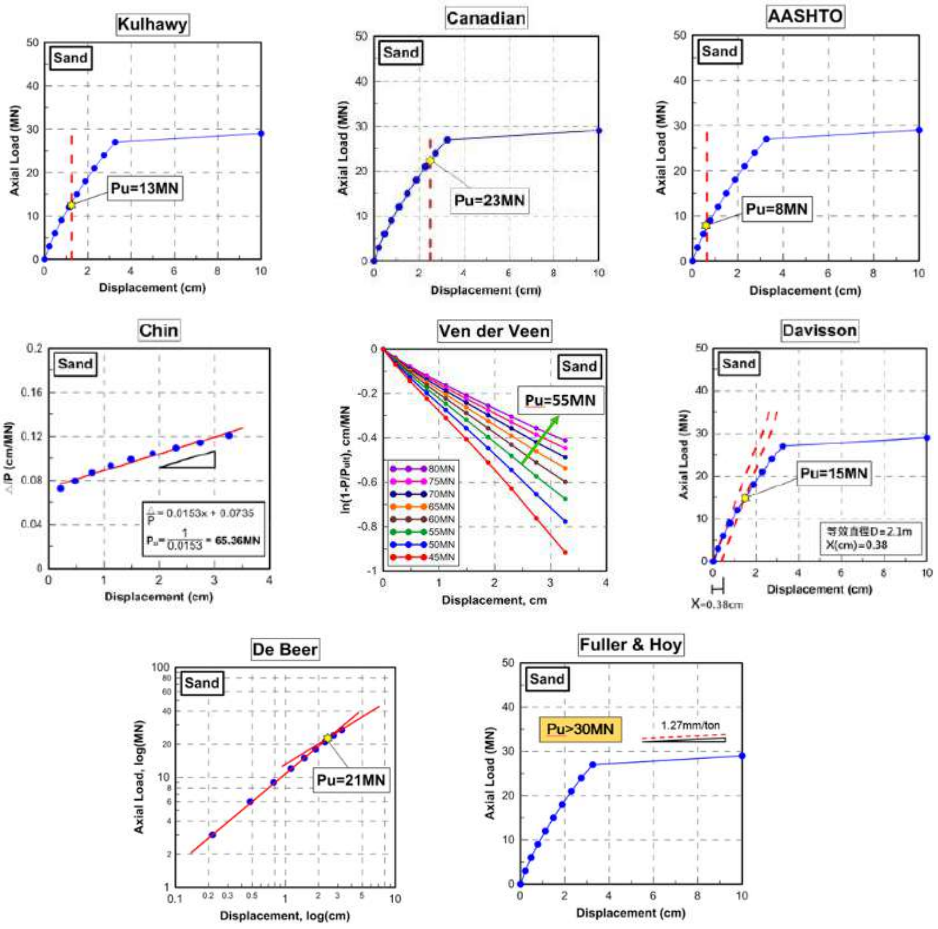

Figure 11 Interpretation of capacity for uplift pile in sands

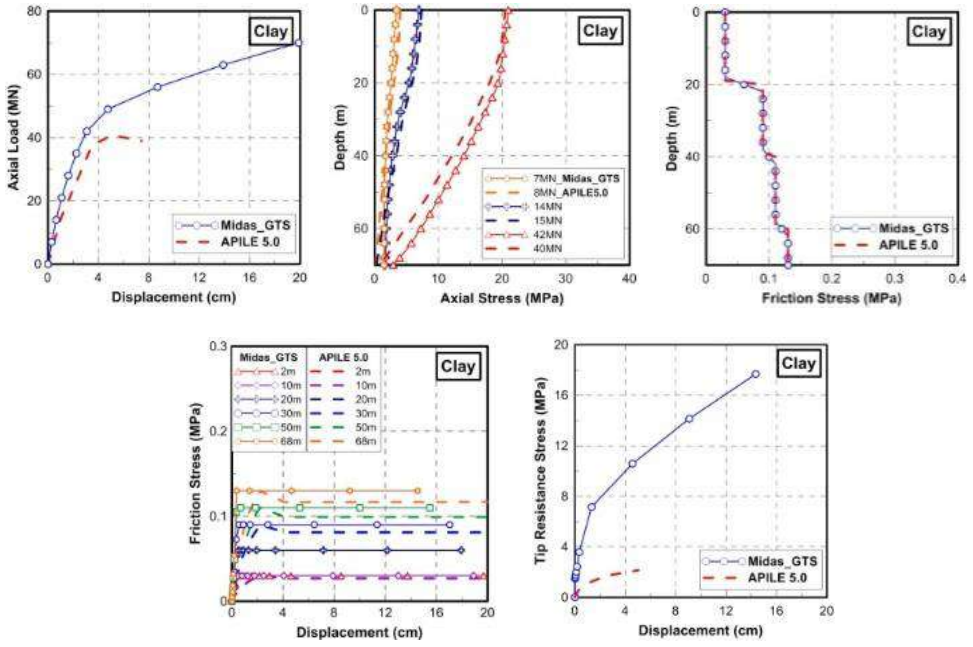

Figure 12 Comparisons of the loading behaviors of compression pile in clays from Midas and APILE analyses

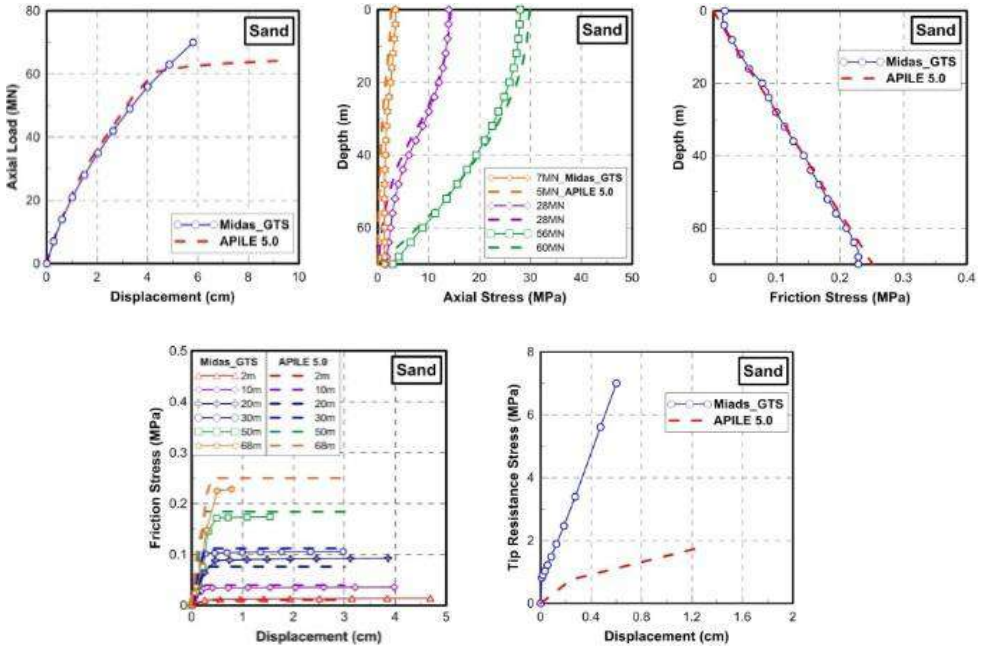

Figure 13 Comparisons of the loading behaviors of compression pile in sands from Midas and APILE analyses

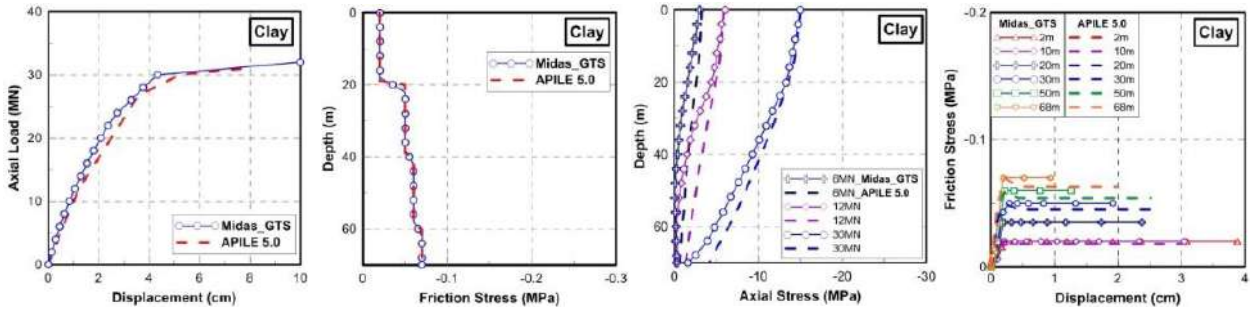

Figure 14 Comparisons of the loading behaviors of uplift pile in clays from Midas and APILE analyses

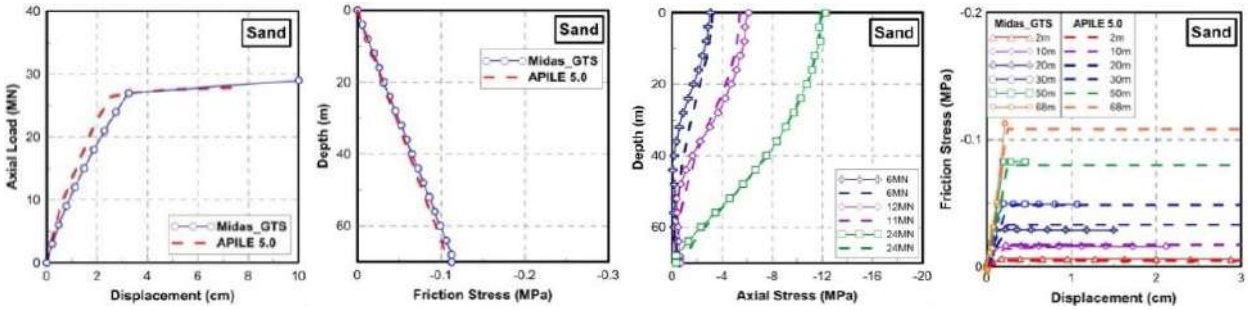

Figure 15 Comparisons of the loading behaviors of uplift pile in sands from Midas and APILE analyses

6. MODELING PILE LOAD TEST DATA

Pile load test data on four barrette piles located in Xingyi district at Taipei Basin (Diagnostic, 2011) were adopted in this study to facilitate the use of the FE analysis with field data. From the bore-hole data, a simplified geological profile with soil parameters was suggested for each case as shown in Table 6. TPCW1 and TPCW2 are the compression piles, whereas TPTW1 and TPTW2 are the uplift piles. Notice that the simplified soil profile consists of interlayer soils of both clays and sands. Details can be found in Wang (2018). The dimensions and material properties of the piles, the dimensions of the analytical zone, and the loading information used in the FE simulations are shown in Table 7. For the uplift piles, again the piles were modeled varying the pile stiffness to simulate the pile damages during the test.

Table 6 Simplified soil profiles for field pile load tests

TPCW1

Layer	Depth (m)	Material Model	Parameters					
			N	E (T/m^2)	ν	γ_t (T/m^3)	Su (T/m^2)	φ'
CL	0-20	Mohr-Coulomb	3	4500	0.4	1.85	4.5	-
CL	20-32		6	8000	0.4	1.85	8	-
CL	32-40		18	12000	0.4	1.88	12	-
SM	40-52		32	10000	0.3	1.95	0	36°
CL	52-59		20	11000	0.35	2.1	11	-
CL	59-64		25	24000	0.35	1.98	24	-
SM	64-69		60	15000	0.3	2.1	0	36°
GW	69-93		>50	41000	0.25	2.19	0	45°

TPCW2

Layer	Depth (m)	Material Model	Parameters					
			N	E (T/m^2)	ν	γ_t (T/m^3)	Su (T/m^2)	φ'
CL	0-20	Mohr-Coulomb	2	3000	0.4	1.85	3.5	-
CL	20-25		4	4500	0.4	1.85	4.5	-
CL	25-32		6	7200	0.4	1.88	9	-
CL	32-35		7	10400	0.35	1.95	13	-
CL	35-40		8	9000	0.4	2.1	9	-
CL	40-47		12	10000	0.35	1.98	10	-
SM	47-52		40	15000	0.3	1.95	0	36°
GW	52-58		>50	35000	0.25	2.19	0	45°
CL	58-78		25	23000	0.35	2.1	23	-

TPTW1

Layer	Depth (m)	Material Model	Parameters					
			N	E (T/m^2)	ν	γ_t (T/m^3)	Su (T/m^2)	φ'
CL	0-20	Mohr-Coulomb	3	4000	0.4	1.85	4	-
CL	20-25		5	5600	0.4	1.85	7	-
CL	25-32		7	6000	0.4	1.88	6	-
CL	32-40		11	8000	0.4	1.85	8	-
CL	40-47		15	13000	0.35	1.98	13	-
SM	47-50		45	20000	0.3	2.1	0	36°
SM	50-53		40	15000	0.3	1.98	0	36°
GW	53-55		>50	35000	0.25	2.19	0	45°
CL	55-62		24	19200	0.35	19.7	24	-
SM	62-70		55	28000	0.3	1.97	23	36°
SM	70-75		57	30000	0.3	1.98	0	36°

TPTW2

Layer	Depth (m)	Material Model	Parameters					
			N	E (T/m^2)	ν	γ_t (T/m^3)	Su (T/m^2)	φ'
CL	0-20	Mohr-Coulomb	2	3000	0.4	1.85	3	-
CL	20-25		4	4500	0.4	1.85	4.5	-
CL	25-32		6	9000	0.4	1.88	9	-
CL	32-35		7	10400	0.35	1.95	13	-
CL	35-40		8	9000	0.4	2.1	9	-
CL	40-47		12	10000	0.35	1.98	10	-
SM	47-52		40	15000	0.3	1.95	0	36°
GW	52-55		>50	35000	0.25	2.19	0	40°
GW	55-58		>50	40000	0.25	2.2	0	45°
CL	58-78		25	23000	0.35	2.1	23	-

Table 7 Numerical model of the pile, analytical zone and the load used for pile load test simulation**s**

Data \ Pile ID	TPCW1	TPCW2	TPTW1	TPTW2
Barrette dimensions	2.6m×1.2m×73m	2.6m×1.2m×58m	2.6m×1.2m×55m	2.6m×1.2m×58m
Young's modulus	Ec=3.35×10^7 kPa	Ec= 3.6×10^7 kPa	0-2m, Ec=7.6×10^6 kPa 2-20m, Ec=1.9×10^7 kPa 20-40m, Ec=3.04×10^7 kPa 40-55m, Ec=3.8×10^7 kPa	0-2m, Ec=7.6×10^6 kPa 2-20m, Ec=1.9×10^7 kPa 20-40m, Ec=3.04×10^7 kPa 40-58m, Ec=3.8×10^7 kPa
Poisson's ratio	0.13			
Dimensions of analytical zone	L×W=60m×60m ; H = pile length + 0~20m to ensure the stability of the solution			
Load type	Compression	Compression	Uplift	Uplift
Load pattern	Maximum load at 7150T, 22 steps, 325T per step was applied	Maximum load at 3850T, 14 steps, 275T per step was applied	Maximum load at 2600T, 20steps, 130T per step was applied	Maximum load at 2600T, 20steps, 130T per step was applied

The simulations using Midas-GTS analysis are shown in Figures 16 and 17 for the piles subjected to compression loads. It can be found the FEA can capture the in-situ pile loading behaviors. The deviations shown in the load-displacement curves are believed to be caused by the constant parameters used throughout the analysis. Nevertheless, the settlements under the maximum loads, the axial and frictional stresses, and the *q-z* curves were found to be in good agreement with the field data. A comparison of the t-z curves from FEA and APILE with the field data for TPCW1 is shown in Figure 18.

For the piles under the uplift load, the results are shown in Figures 19 and 20. Similar comparisons can be found for load-displacement curves, axial and frictional stress along the piles, however for the *t-z* curves, it can be found that the in-situ data are difficult to simulate. See Figure 21 for t-z curves of the TPTW1 pile. The progressive damage of the pile under the tensile loads were modeled inadequately using a degraded stiffness applied to the pile, and treating them as constant throughout the analysis.

Again, the comparisons on the pile capacities from the interpretations using the numerical load-displacement curves from FEA as well as the bearing capacity equations and the APILE analysis were made and the results are shown in Tables 8 and 9.

Corresponding graphic results are shown in Figures 22 and 23 for TPCW1 and TPTW1 piles. Notice that since the soil profiles were inter layered soils consisting of clays and sands, the bearing capacities were calculated using different methods and the averaged values were reported. Details of the calculations can be found in Wang (2018). It was found that the estimations from a number of the interpretations

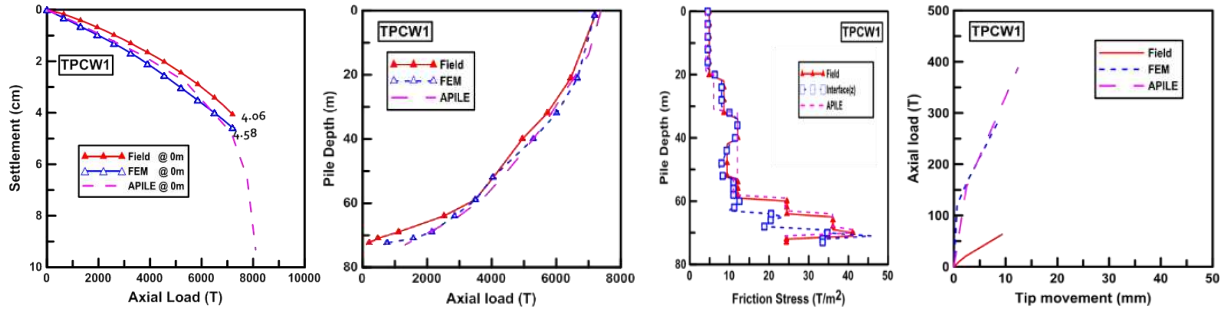

Figure 16 Comparisons of the loading behaviors of TPCW1bareette pile from Midas and APILE analyses

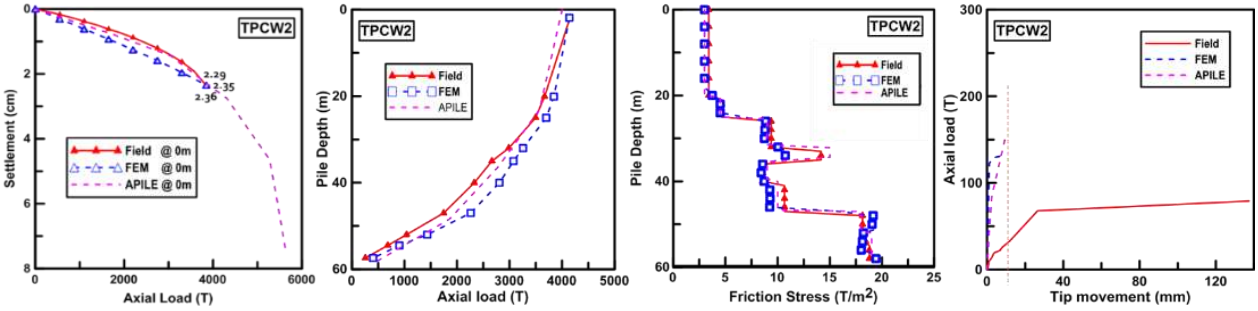

Figure 17 Comparisons of the loading behaviors of TPCW2 barrette pile from Midas and APILE analyses

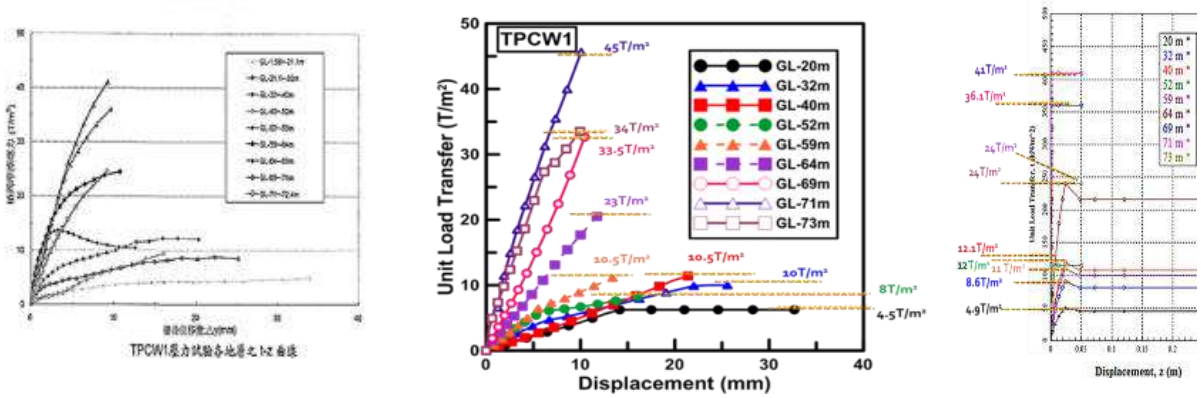

Figure 18 Comparisons of the t-z curves for TPCW1 barrette pile from field measurement, Midas and APILE analyses

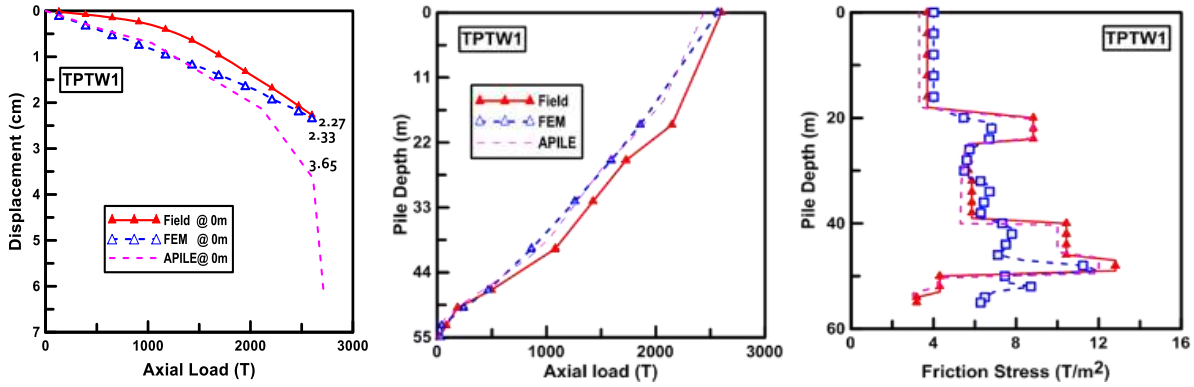

Figure 19 Comparisons of the loading behaviors of TPTW1 barrette pile from Midas and APILE analyses

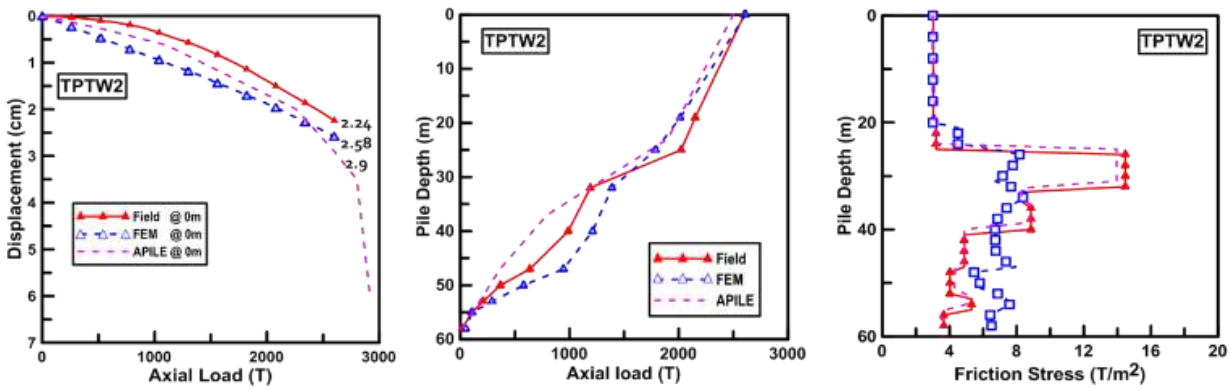

Figure 20 Comparisons of the loading behaviors of TPTW2 barrette pile from Midas and APILE analyses

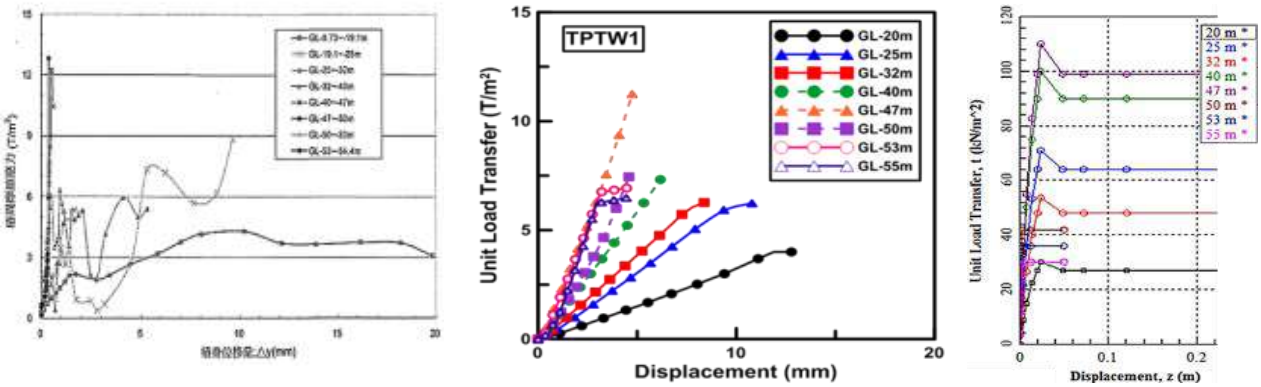

Figure 21 Comparisons of the t-z curves for TPTW1 barrette pile from field measurement, Midas and APILE analyses

Table 8 Pile capacities calculated from analytic equations for the testing piles

TPCW1

Sand \ Clay	α method – Q (MN)	λ method – Q (MN)	AASHTO - Q (MN)
Meyerhof - Q (MN)	97.16	111.32	97.04
AASHTO - Q(MN)	102.32	116.48	102.20
Averaged Q_{ult} (MN)	104.42		

TPCW2

Sand \ Clay	α method - Q (MN)	λ method - Q (MN)	AASHTO - Q (MN)
Meyerhof - Q (MN)	76.99	90.44	75.83
AASHTO - Q (MN)	79.44	92.88	78.27
Averaged Q_{ult} (MN)	82.31		

TPTW1

Sand \ Clay	Das and Seeley - Q (MN)	AASHTO - Q (MN)
Meyerhof and Adam – Q (MN)	16.19	13.74
AASHTO - Q (MN)	16.14	13.68
Averaged Q_{ult} (MN)	14.94	

TPTW2

Sand \ Clay	Das and Seeley - Q (MN)	AASHTO - Q (MN)
Meyerhof and Adam – Q (MN)	16.14	14.01
AASHTO - Q (MN)	16.09	13.95
Averaged Q_{ult} (MN)	15.05	

Table 9 Pile Capacities estimated from interpretation methods, analytic equations and APILE analysis

TPCW1

Interpretation method	O_{ult} (MN)	Interface Frictions, Q (MN)	Averaged Q_{ult} (MN) from cap. equations	APILE O_{ult} (MN)
Terzaghi	**>130**	**111.69**	**104.42**	**99.58**
Canadian	**46**			
AASHTO	**15**			
Chin	**330**			
Van der Veen	**96**			
Davisson	**93**			
De Beer	**50**			
Fuller and Hoy	**>130**			

TPCW2

Interpretation method	O_{ult} (MN)	Interface Frictions, Q (MN)	Averaged Q_{ult} (MN) from cap. equations	APILE O_{ult} (MN)
Terzaghi	**>82.5**	**86.30**	**82.31**	**75.21**
Canadian	**40**			
AASHTO	**12**			
Chin	**200**			
Van der Veen	**90**			
Davisson	**73**			
De Beer	**48**			
Fuller and Hoy	**>82.5**			

TPTW1

Interpretation method	O_{ult} (MN)	Interface Frictions, Q (MN)	Averaged Q_{ult} (MN) from cap. equations	APILE O_{ult} (MN)
Canadian	**27**	**29.5**	**14.94**	**23.47**
AASHTO	**9**			
Chin	**143**			
Van der Veen	**N/A**			
Davisson	**27**			
De Beer	**30**			
Fuller and Hoy	**>39**			

TPTW2

Interpretation method	O_{ult} (MN)	Interface Frictions, Q (MN)	Averaged Q_{ult} (MN) from cap. equations	APILE O_{ult} (MN)
Canadian	**26**	**28.31**	**15.05**	**24.66**
AASHTO	**7**			
Chin	**143**			
Van der Veen	**N/A**			
Davisson	**26**			
De Beer	**30**			
Fuller and Hoy	**>39**			

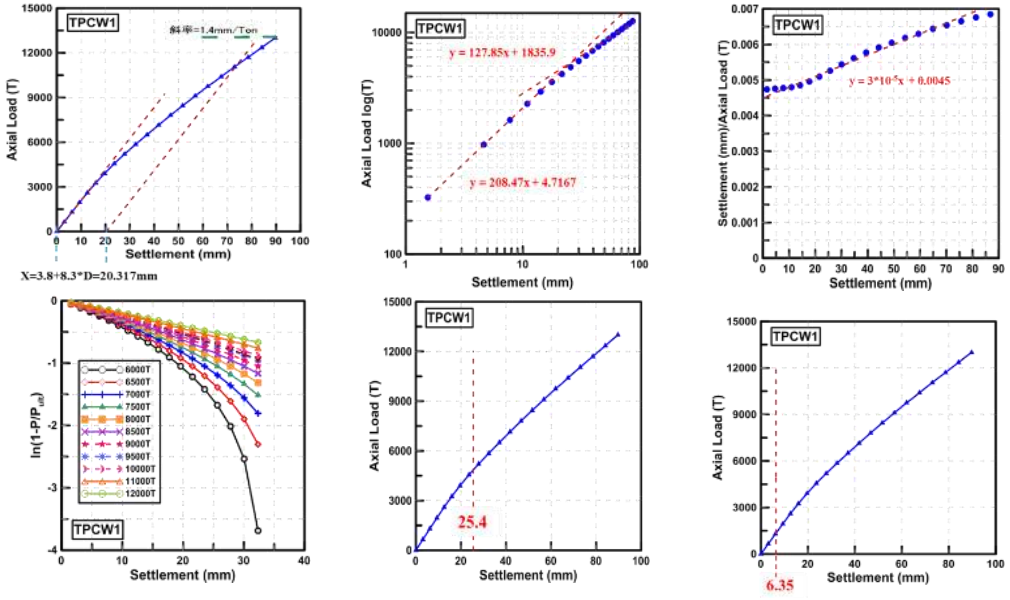

Figure 22 Graphic interpretations on pile capacities of TPCW1 barrette pile

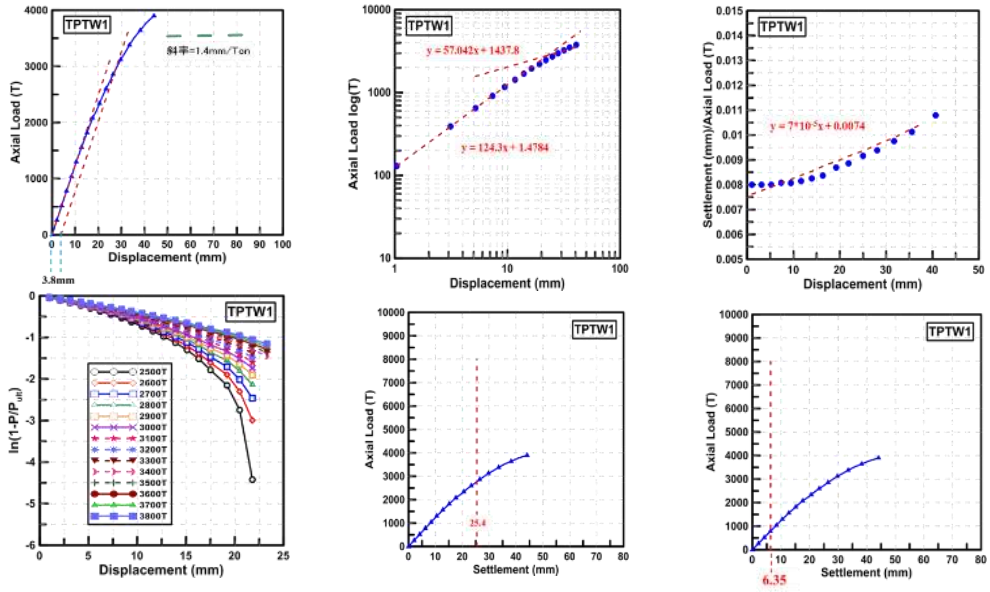

Figure 23 Graphic interpretations on pile capacities of TPTW1 barrette pile

based on the numerical solutions are within rational agreements with those obtained from the bearing capacity equations for compression piles. However, the estimations from the capacity equations were found to be much less than the applicable predictions for the uplift piles. The coefficients used to reduce the strength parameters in the capacity equations for uplift piles seem to be smaller for soft clays in the Taipei Basin.

7. CONCLUDING REMARKS

This study presents examples of using a three-dimensional FEA to model barrette piles which have been subjected to compression and uplift loads. Comparisons were made using a similar APILE analysis. Capacities of the model piles were estimated using the interpretation methods and analytic equations for the bearing capacity of pile. Investigations were also carried out on the pile load test data. Again, the pile capacities reported were compared to those calculated from the bearing capacity equations and APLIE analysis. The following conclusions were drawn from this study.

1) The effects of the rectangular shape of the barrette pile were found insignificant to the stresses and deformations distributed at the same cross-section plane of the pile. The bearing capacity equations are able to predict the capacities of the barrette pile in clays, while under the influence of either compression or uplift loads. The Canadian method, Davisson method and De Beer method were all found to produce closer predictions. For the compression pile in sands, the Meryerhof equation, which provides the lowest as compared to the other calculations, was found to produce similar results to the interpretations using Davisson method and De Beer method. The other calculations were found closer to the results suggested by Van der Veen method. For the case of the uplift pile in sand, the variations in the calculation results became less. The Canadian method and De Beer method provide the best approximations.

2) The model parameters of the interface element are important to barrette piles subjected to both compression and uplift loads. For piles in sandy soils, if the roughness of the interface between pile and soil exists, apparent resistance can be found at the pile head. The frictions between the pile and soils will be affected by both the friction angle of the sand and the roughness of the pile-soil interface.

3) For compression piles, three-dimensional FEA can provide better completeness of load-displacement curves than the one-dimensional FDA does. Such an advantage could facilitate the applicability of the interpretation methods when launching the field data using FE analysis. As to the uplift pile, both FEA and FDA can provide similar results.

4) The pile capacities obtained from the interpretation methods and those calculated from the bearing capacity equations were found to be rationally comparable. The reductions of the soil parameters to simulate the frictions between the pile and the soils needs further attention, especially with regards to the barrette pile in soft clays in order to maintain a rational design.

5) For the interpretation methods used to predict the capacities of barrette piles located in the Taipei Basin, for the inter layered soils, Davisson method and Van der Veen Method, can provide closer results to the bearing capacity equation for the cases under compression load. For uplift load case, the damages which occur in the pile causes difficulty in simulations. It was noted that the Canadian method, Davisson method and De Beer method can provide a similar prediction to those obtained by interface frictions and APILE. Using a 50% reduction of the frictions for the compression pile in clays, to simulate the frictions for the uplift pile in the bearing capacity equation, seems to provide an overly conservative estimation.

8. ACKNOWLEDGEMENTS

The paper presents partial results of the research study funded by Ground Master Construction/MICE Engineering Consultants, Taiwan. Sincere gratitude is acknowledged. Great appreciation is extended to Diagnostic Engineering Consultants Co., Ltd., Taiwan for the pile load test data provided to this study.

9. REFERENCES

American Association of State Highway and Transportation Officials, AASHTO (2002) Standard Specifications for Highway Bridges. 17edit.

Abderlrazaq, A., Badelow, F., Sung, H.K., and Poulos, H.G. (2011) ″Foundation design of the 151 story Incheon Tower in a reclamation area.″. Geotechnical Engineering, SEAGS and AGSSEA, 42(2), 85-93.

Canadian Geotechnical Society (1985) Canadian Foundation Engineering Manual, 2nd Edit. BiTech Publishers Ltd., Vancouver, Canada, 456p.

Chang, D.W., Lee, M.R., M.Y. Hong and Y.C. Wang (2016) "A simplified modeling for seismic responses of rectangular foundation on piles subjected to horizontal earthquakes". J. of GeoEngineering, TGS, 11(3), 109-121.

Chang, D.W., Lien, H.W., and Wang, T. (2018) "Finite difference analysis of vertically loaded raft foundation based on the Plate Theory with boundary concern". Journal of GeoEngineering, TGS, 13(3), 135-147.

Chang, D.W. and Lien, H.W. (2018) "Finite difference analysis for combined pile raft foundations under vertical loads", The Sixteen Asian Regional Conf. on Soil Mechanics and Geotechnical Engineering, October 14-18, Taipei, Taiwan (under preparation).

Chang, D.W., Roesset, J.M. and Wen, C.H. (2000) "A time-Domain viscous damping model based on frequency-dependent damping ratios". Soil Dynamics and Earthquake Engineering, 19, 551-558.

Chang, D.W. and Yeh, S.H. (1999) "Time-domain wave equation analysis of single piles utilizing transformed radiation damping". Soils and Foundations, Japanese Geotechnical Society, 39(2), 31-44.

Chang, Y. L. (1937) Discussion on "Lateral pile-loading tests" by LB Feagin. Transaction of ASCE. 102, 272-278.

Chin, F.K.. (1970) "Estimation of ultimate load of piles not carried to failure", Procds., 2nd Southeast Asian Conf. on Soil Eng., 81-90

Das, B.M. and Seeley, G.R. (1982) "Uplift capacity of pipe piles in saturated clay", Soils and Foundations, JGS, 22(1), 91-94.

Davisson, M.T. (1972) "High capacity piles", Proceedings, Lecture Series, Innovations in Foundation Construction, ASCE, Illinois Section.

De Beer, E.E. (1967) "Proefonder vindelijke Bildrage Tot De Studie Van Het Grensdraag Vermogen Van Zang Onder Funderingen on Staal", Tijdshrift der Openbar Weken van Belgie, Nos. 6-67 and 1-,4-,55, 6-68.

Diagnostic Engr. Co. (2011) Static Pile Load Test Report – Preliminary Planning of Super Dorm Stadium in Taipei (in Chinese).

Wang, S.T., Arrellaga J.A. and Vasquez L.G. (2018) APILE User's Manual, Ensoft, Inc., TX, USA.

Isenhower, W.M., Wang, S.T. and Vasquez, L.G. (2018) LPILE User's Manual, Ensoft, Inc., TX, USA.

Fellenius, B.H. (1980) "The analysis of results from routine pile load test". Ground Engineering, Foundation Publication Ltd., London, 13(6), 19-31.

Fellenius, B.H. (1984) "Negative skin friction and settlement of piles", Proceedings of the Second International Seminar, Pile Foundations, Nanyang Technological Institute, Singapore, 18 p.

Fellenius, B.H. (1989) "Unified design of piles and pile groups", Transportation Research Board, Washington, TRB Record 1169, pp. 75 - 82.

Fellenius, B.H. (1998) "Recent advances in the design of piles for axial loads, dragloads, downdrag, and settlement", Proceedings of a Seminar by American Society of Civil Engineers, ASCE, and Port of New York and New Jersey, April 1998, 19 p.

Fellenius, B.H. (1999a) Basics of Foundation Design. Second expanded edition. BiTech Publishers, Vancouver, 140 p.

Fellenius, B.H. (1999b) "Bearing capacity- A delusion?", Proceedings, Deep Foundation Institute 1999 Annual Meeting, Dearborn, Michigan, October 14 -16.

Fuller, R.M. and Hoy, H.E. (1970) "Pile load test including quick-load test method, Conventional Methods and Interpretations". Highway Research Record 333, pp. 1-30.

Hirany, A. and Kulhawy, F.H. (1988) "Conduct and Interpretation of Load Tests on Drilled Shaft Foundations: Detailed Guidelines", Report. EL-5915(1), Electric Power Research Institute, Palo Alto.

Hsu, M.C. (2017) The Bearing Behavior of Barette Piles under Vertical Loading, Doctoral Dissertation, Dept. of Civil Engineering, National Taiwan University (in Chinese).

Lin, C. (2018) Numerical Analysis on Barrette Pile Bearing Mechanism under Vertical Loading, Master Thesis, Dept. of Civil Engineering, Tamkang University (in Chinese).

Meyerhof, G.G. (1976) "Bearing capacity and settlement of pile foundations". Journal of Geotechnical Engineering Division, ASCE, 102(GT3), 197-228.

Meyerhof, G.G. and Adams, J.I. (1968) "The ultimate uplift capacity of foundation". Canadian Geotechnical Journal, CGS, 5(4), 225-244.

Midas (2014) Midas GTS NX User Manual, Midas IT Co.

Poulos, H.G. (2001) ″Pile-raft foundation: design and applications". Geotechnique, 51(2), 95-113.

Terzaghi, K. (1942) "Discussion of the progress report of the committee on the bearing value of pile foundations" Proc., ASCE, Vol. 68.

Tomlinson, M. J. (1971)" Some effects of pile driving on skin friction", Conference on Behaviour of Piles, London, 107-114.

Van der Veen, C. (1953) "The bearing capacity of a pile", The 3rd International Conference on Soil Mechanics and Foundation Engineering, 84-90.

Vijayvergiya, V.N. and Focht, Jr., J.A. (1972) "A new way to predict capacity of piles in clay", 4th Offshore Technology Conference, Houston, OTC paper 1718.

Wang, T.Y. (2018) Analysis of Pile Load Test Data of Barrette Piles, Master Thesis, Dept. of Civil Engineering, Tamkang University (in Chinese).